



Novel insights into global translational regulation through Pumilio family RNA-binding protein Puf3p revealed by ribosomal profiling

Zhe Wang^{1,2} · Xuepeng Sun³ · Josephine Wee¹ · Xiaoxian Guo¹ · Zhenglong Gu¹

Received: 25 May 2018 / Revised: 16 June 2018 / Accepted: 19 June 2018 / Published online: 27 June 2018
© Springer-Verlag GmbH Germany, part of Springer Nature 2018

Abstract

RNA binding proteins (RBPs) can regulate the stability, localization, and translation of their target mRNAs. Among them, Puf3p is a well-known Pumilio family RBP whose biology has been intensively studied. Nevertheless, the impact of Puf3p on the translational regulation of its downstream genes still remains to be investigated at the genome-wide level. In this study, we combined ribosome profiling and RNA-Seq in budding yeast (*Saccharomyces cerevisiae*) to investigate Puf3p's functions in translational regulation. Comparison of translational efficiency (TE) between wild-type and *puf3Δ* strains demonstrates extensive translational modulation in the absence of Puf3p (over 27% genes are affected at the genome level). Besides confirming its known role in regulating mitochondrial metabolism, our data demonstrate that Puf3p serves as a key post-transcriptional regulator of downstream RBPs by regulating their translational efficiencies, indicating a network of interactions among RBPs at the post-transcriptional level. Furthermore, Puf3p switches the balance of translational flux between mitochondrial and cytosolic ribosome biogenesis to adapt to changes in cellular metabolism. In summary, our results indicate that TE can be utilized as an informative index to interrogate the mechanism underlying RBP functions, and provide novel insights into Puf3p's mode-of-action.

Keywords Post-transcriptional regulation · Puf3 · Ribosomal profiling

Communicated by M. Kupiec.

Zhe Wang and Xuepeng Sun contributed equally

Electronic supplementary material The online version of this article (<https://doi.org/10.1007/s00294-018-0862-4>) contains supplementary material, which is available to authorized users.

✉ Zhe Wang
zhw2001@med.cornell.edu

✉ Zhenglong Gu
zg27@cornell.edu

¹ Division of Nutritional Sciences, Cornell University, 312 Savage Hall, Ithaca, NY 14853, USA

² Division of Infectious Diseases, Weill Medical College of Cornell University, 413 E 69th St, New York, NY 10021, USA

³ Boyce Thompson Institute, Ithaca, NY 14853, USA

Introduction

The concept of RNA regulons was proposed to specifically describe the observation that mRNA-binding proteins (RBPs) usually bind and orchestrate the fate of target mRNAs encoding functionally related proteins (Keene 2007). It is increasingly clear that RNA regulons play an important role in determining the stability, subcellular localization, and translation of their targets, and thus are essential for phenotypic outcomes and even disease states in various organisms including humans (Blackinton and Keene 2014; Imig et al. 2012; Celik et al. 2017; Defenouillère and Fromont-Racine 2017; Evans and Ling 2017). The Pumilio family of proteins are a group of RBPs that are structurally conserved but functionally divergent from yeast to mammals (Wickens et al. 2002; Zhang et al. 1997; Wang et al. 2002; Kennedy et al. 1997). One of the most well-studied examples, Puf3p, specifically recognizes and binds a group of mRNA transcripts with the characteristic motif “CHTGTAWATA” in their 3' untranslated region (3'UTR) (Olivas and Parker 2000; Gerber et al. 2004). Puf3p has been extensively studied for its unique function as a critical

post-transcriptional regulator for maintaining efficient intracellular energy production via respiration, especially in conditions where only non-fermentative carbon sources exist (Miller et al. 2014; Lee and Tu 2015; Eliyahu et al. 2010).

Several biochemical approaches have been employed to study Puf3p's mechanism of action as an RBP. For example, in yeast, Puf3p interacts with the 3' UTR of *COX17* and results in rapid deadenylation of the mRNA molecule, subsequently increasing the *COX17* decay rate (Jackson et al. 2004; Houshmandi and Olivás 2005; Lee et al. 2010; Miller et al. 2014). Above mode-of-action involves the recruitment of the Ccr4p–Pop2p–Notp deadenylation complex to *COX17* mRNA by direct interaction of Puf3p with Ccr4p (Lee et al. 2010). Others have also shown that the interaction between Puf3p and its target mRNAs can aid in trafficking of selected mRNAs to the surface of the mitochondrion for translating mitochondrial proteins (Eliyahu et al. 2010; Gadir et al. 2011). Most recently, it was reported that Puf3p's activity could be regulated by phosphorylation during glucose depletion (Lee and Tu 2015). As a means to promote energy efficiency, Puf3p binds specifically to the 3'UTR of nuclear-encoded mitochondrial genes required for respiration and causes these transcripts to be compartmentalized around the Electron Transfer Chain (ETC). Above findings thus suggest the key functional roles of Puf3p at the post-transcriptional level. Puf3p was also used as the first example to investigate the evolution of an RBP gene regulatory network (Jiang et al. 2010, 2014).

Much has been learned about the function of RBPs from genetic approaches, phenotypic studies, RBP immunoprecipitation microarrays, and evolutionary analyses (Gerber et al. 2004; Imig et al. 2012; Mittal et al. 2011; Scherrer et al. 2010; Riordan et al. 2011). Given that RBPs are involved in post-transcriptional regulation, an improved understanding of how RBPs affect translation at the genome level will lead to a better understanding of their functional roles in biology. Ribosome profiling (Ribo-Seq) is a powerful tool which can provide the most direct readout of the intracellular translation state of a transcript, including information on the location of translation start/stop sites, ribosome distribution pattern, and the moving rate of the translating ribosome (Ingolia et al. 2009, 2013; Morris 2009). Previous studies using ribosomal profiling have suggested that translational efficiency (TE) is an informative index to evaluate whole genome translational activity (Pop et al. 2014; Brar et al. 2012). In the case of Puf3p, this index becomes especially valuable when adapted to analyze specific genes that are targets of Puf3p translational regulation.

Here, we combined Ribo-Seq and RNA-Seq approaches to systematically examine the biological function of *S. cerevisiae* Puf3p in regulating mRNA abundance and translation activity when growing on non-fermentative carbon sources. Our results indicate that Puf3p is a key regulator of

a post-transcriptional network of RBPs. Furthermore, our observations suggest that Puf3p plays an important role in regulating the TE of key metabolic enzymes in central carbon metabolism. We also found that the absence of Puf3p decreased the TE of a subset of genes encoding mitochondrial ribosome subunits, but surprisingly up-regulated TE of cytosolic ribosome subunits, an observation offering new insights into the mode-of-action of Puf3p as a molecular switch to regulate the translational flux balance between mitochondrial and cytosolic ribosome biogenesis. Meanwhile, our results revealed an increased probability of protein–protein interaction among Puf3p's targets, suggesting that Puf3p may synchronize the TE of its targets to aid in the formation of specific protein complexes. In conclusion, our survey of Puf3p's mode-of-action using ribosomal profiling demonstrates its essential functional role in regulating cellular energy homeostasis at the translational level.

Results

Puf3p regulates global translation of genes at the genome-wide level

Earlier studies have reported specific biological functions of Puf3p under various nutrient conditions (Miller et al. 2014; Gupta et al. 2014; Rowe et al. 2014). In addition, the genetic knockout of *S. cerevisiae* Puf3p leads to a dramatic growth inhibition when yeasts are cultured under respiratory conditions utilizing ethanol as sole carbon source (Jiang et al. 2010; Lee and Tu 2015). To further understand the role of Puf3p in the modulation of cellular respiration, we adopted Ribo-Seq and RNA-Seq approaches to investigate how gene transcription and translation are regulated by Puf3p in *S. cerevisiae* grown under non-fermentative growth conditions (Yeast Extract–Peptone–Ethanol–Glycerol medium, abbreviated as YPEG) where the growth is delayed for the Puf3 mutants (Supplementary Fig. 1). The overall experimental workflow and statistical analyses are shown in Fig. 1, and duplicate biological samples were collected for both Ribo-Seq and RNA-Seq. Our results revealed high correlation between biological replicates (Pearson correlation: ~0.98 for Ribo-Seq and ~0.99 for RNA-Seq in wild-type samples; ~0.99 and ~0.99, respectively, in *puf3Δ* samples), and robustness of the Ribo-Seq dataset: reads were peaked between 27–29nt, a size close to the length of RNA footprint in yeast (~28nt in yeast), and typical characteristics of Ribo-Seq reads were observed in our data (Ingolia et al. 2009) (Supplementary Figs. 2, 3 and 4).

To identify specific genes with differential RNA abundance and translational activities that are dependent on Puf3p's mode-of-action, we compared mRNA and Ribosome Footprinting (RFP) abundances between wild-type

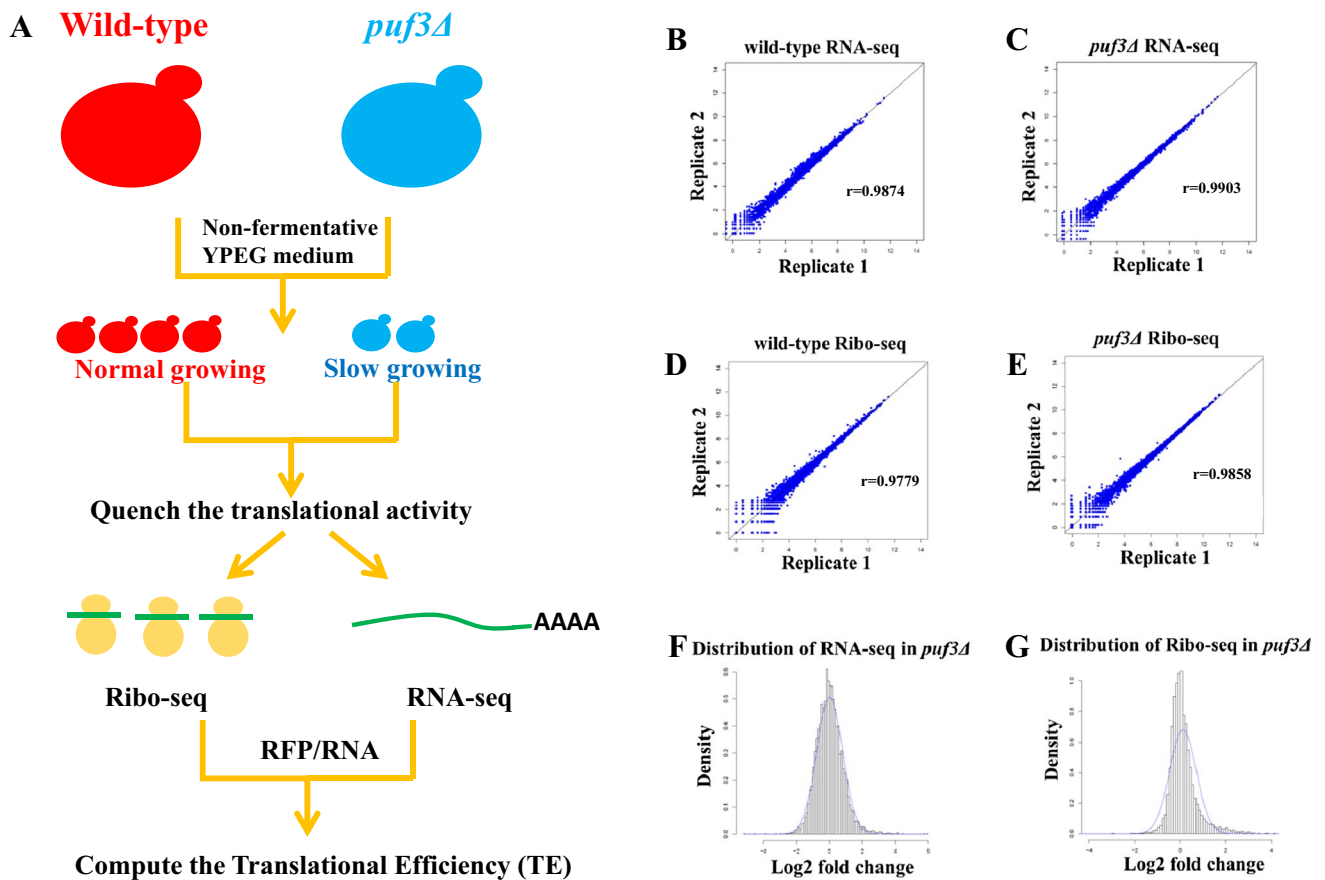


Fig. 1 The workflow of ribosomal footprint profiling and overall statistical analysis. **a** The workflow of the experimental design. Two yeast strains (WT and *puf3Δ*) were cultured in YPEG to mid-log phase. The whole-genome translation was stopped by addition of cycloheximide (CHX) followed by division of cell pellets into two parts, one for RNA-Seq, and the other for Ribo-Seq (for details, see Methods). Raw sequencing reads were cleaned and mapped to the yeast genome for further analyses. **b** The correlation coefficient of

two biologically replicated RNA-Seq samples for wild-type yeast. **c** The correlation coefficient of two biologically replicated RNA-Seq samples for *puf3Δ* yeast. **d** The correlation coefficient of two biologically replicated Ribo-Seq samples for wild-type and yeast. **e** The correlation coefficient of two biologically replicated Ribo-Seq samples for *puf3Δ* yeast. **f** The distribution of relative mRNA abundance changes in *puf3Δ* yeast. **g** The distribution of relative RFP abundance changes in *puf3Δ* yeast

and *puf3Δ* strain utilizing a negative binomial model-based method introduced by Anders and Huber (Anders and Huber 2010). We applied the criteria of adjusted p-value (Benjamini-Hochberg method) ≤ 0.05 and $|\log_2(\text{fold change})| \geq 1.0$ to the data. A total of 1109 out of 6575 genes analyzed (~17%) showed significant RNA abundance variation between wild-type and *puf3Δ* strains grown in YPEG, of which 620 genes were up-regulated, and 489 genes were down-regulated (Table 1). Using the same criteria, we found that 496 genes showed significant RFP changes, of which 446 genes were up-regulated, but only 50 genes were down-regulated. When Translation Efficiency (TE) was used as an index to quantify the efficiency of translational machinery, the TE for 1785 genes (increased for 1007 genes, decreased for 778 genes) was significantly altered in the absence of Puf3p. The detailed fold changes and statistical analyses for individual genes regarding RNA abundance,

RFP abundance, and TE can be found in Supplementary Tables 1 and 2. We also compared the transcription/translation profiles of wild-type yeast in YPEG medium and in YPD medium (Supplementary Fig. 5). Among the genes with TE changes, the Puf3p's target, such as *COX17*, shows a relatively higher TE in YPEG medium, consistent to its essential role in respiration, as a copper metallochaperone involved in cytochrome c oxidase function.

We compared our data with several previous published studies of Puf3p. In an earlier study, Kershaw et al. reported that Puf3p only impacted dozens of genes at mRNA level although it has about 1000 binding targets (Kershaw et al. 2015). As shown in Supplementary Fig. 6, there are over 91% overlapped Puf3p upregulated genes between our RNA-Seq dataset, suggesting that the Puf3p's binding capacity is possibly carbon source unrelated. We next compared our TE datasets with three sets of Puf3p's binding list (achieved by

Table 1 Overall impact of Puf3p KO on transcription, translation and TE

	Upregulated in <i>puf3Δ</i>	Down-regulated in <i>puf3Δ</i>
RNA-Seq		
All genes list	620	489
Binding targets-Gerber list	31	2
Binding targets-Kershaw list	127	60
Binding targets-Freeberg list	86	33
Ribo-Seq		
All genes list	446	50
Binding targets-Gerber list	8	2
Binding targets-Kershaw list	38	5
Binding targets-Freeberg list	23	5
TE		
All genes list	1007	778
Binding targets-Gerber list	8	55
Binding targets-Kershaw list	133	183
Binding targets-Freeberg list	56	125

“All genes list” shows the number of regulated genes at the whole-genome scale. “Binding target” shows the number of regulated genes that were direct Puf3p target genes in previous reports

RIP-Chip, RIP-Seq, and PAR-CLIP, respectively) (Gerber et al. 2004; Kershaw et al. 2015; Freeberg et al. 2013). As shown in Supplementary Fig. 7 interestingly, all of these three sets of Puf3p’s binding target lists show very similar overlapped ratios with our changed TE gene list: Gerber data is 28.6%, Kershaw data is 27.9%, and Freeberg data is 30.2%. This result supports a good reproducibility among three different genomic assays for capturing RNA–Protein interaction. The result also shows that the majority of Puf3p’s binding list (about 70%) is not affected at the translational level, which may be more related to mRNA stability controlling, mRNA localization or other unknown molecular functions of Puf3p. Supplementary Fig. 8 and Supplementary Table 3 show the overlaps and their Δ TEs

Table 2 The GO (gene ontology) functional analysis of Puf3p-regulated genes

	Enriched functional categories	<i>P</i> value
Genes with decreased TE in <i>puf3Δ</i>	mRNA binding	2.51E–18
	oxidoreductase activity	5.2E–12
	peptidase activity, acting on L-amino acid peptides	0.0000282
	phosphotransferase activity, alcohol group as acceptor	0.00197
	isocitrate dehydrogenase activity	0.00724
Genes with increased TE in <i>puf3Δ</i>	N/A	N/A

The analysis was conducted in Gene Ontology Term Finder in Saccharomyces Genome Database (<http://www.yeastgenome.org/cgi-bin/GO/goTermFinder.pl>). The categories with *P* value < 0.01 are listed

N/A means not available

of the reported Puf3p binding targets. Finally, we analyzed the abundances of *COX17* and other known Puf3p targets in our dataset. As shown in Supplementary Fig. 9, we found that most of the Puf3p targets have the increased mRNA abundances but decreased TE values in *puf3Δ* strain (except *MRS1*). Although the mechanism of Puf3p’s divergent impact on mRNA stability and mRNA translation is still unclear, we guess that other factors, such as some Puf3p’s protein interactor(s), as well as the phosphorylation event of Puf3p, may take part in the elegant controlling Puf3p’s functional role.

Puf3p is a key regulator of a post-transcriptional network of RBPs

Genes with increased TEs could not be grouped into any enriched functional category based on the GO-term analysis (*p* value $\leq 1E-2$; Table 2) using software GO Term Finder. However, genes with decreased TEs were associated with several specific functional roles. Above pathway enrichment pattern was also confirmed when we used the TE changed Puf3p’s binding targets as an input (Supplementary Tables 4, 5 and 6). The results are also largely overlapped by the read-out from the analysis using another software Genecodis (Supplementary Table 7). Among them, interestingly, the most significant category is for genes with mRNA binding activity (GO: 0003729). As shown in Table 2, there are 65 RBPs that are affected by Puf3p at the translational level, compared to a total of 172 mRNA binding protein genes annotated in the GO analysis, and this enrichment is highly significant (*P* value = 2.51E–18).

This observation motivated us to build a relation tree based on these RBPs’ functions. As shown in Fig. 2, these genes participate in diverse processes related to mRNA fates, including mRNA splicing, mRNA decay, mRNA localization and mRNA translation. We analyzed the 3’UTR (defined as up to 500 bp downstream from the stop codon) for canonical Puf3p binding sites (P3E). Among the 65 RBP genes, 17 RBPs have at least one P3E in their 3’UTR,

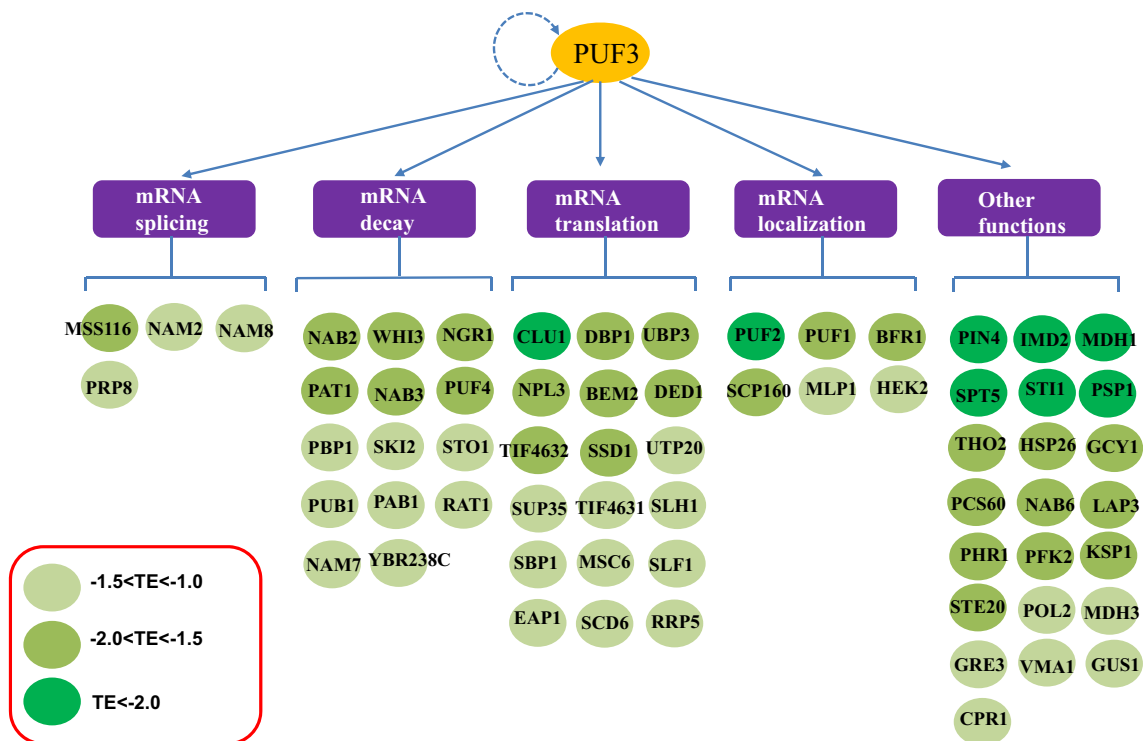


Fig. 2 Puf3p is a key regulator of a post-transcriptional network of RBPs. Genes whose TE is regulated by Puf3p are mostly enriched in RNA-binding functions (Table 2). The downstream RBPs are

grouped by similar molecular functions based on GO terms. The color-barcode represents the extent of ΔTE value. The dashed line represents the computationally annotated self-regulation of Puf3p

indicating that they may be direct targets of Puf3p in our experimental conditions. Significantly, earlier experiments that identified Puf3p targets were performed using glucose as carbon source, which may not have shown Puf3p’s major functional roles in cellular respiration. It is also worth noting that the 3’UTR of *PUF3* also contains a P3E, suggesting that Puf3p might be self-regulated as part of a feedback loop mechanism. Another noteworthy hit is *SLF1*, which as reported links to mitochondrial translation and oxidative phosphorylation (Chatenay-Lapointe and Shadel 2011). In together, these results demonstrate that Puf3p could serve as a post-transcriptional master regulator affecting the TE of other RBPs, and hundreds of their downstream targets.

Puf3p plays an important role in regulating intracellular energy homeostasis

Yeast cells utilize the evolutionary conserved central carbon metabolism (CCM) modules, including glycolysis and the tricarboxylic acid (TCA) cycle, to break down different carbon sources from the environment. To further explore the mechanism of Puf3p in mitochondrial function, we supplied glycerol and ethanol as carbon sources in liquid medium. Puf3p shows extensive regulation of CCM at the TE level, demonstrated by the overall regulatory patterns of

Puf3p on central carbon metabolism (Fig. 3). First, we found that almost all of the key enzymes in glycolysis and pentose phosphate pathway show down-regulated TEs in *puf3Δ* strain. For example, in glycolysis/glycogenesis pathway, the relative TE are 37.4% for *GLK1* (Glucokinase), 39.8% for *PGI1* (Phosphoglucose Isomerase), 39.1% for *FBA1* (Fructose 1,6-Biphosphate Aldolase), 36.6% for *GLD1* (Glycer-aldehyde-3-Phosphate Dehydrogenase), 25.9% for *PGK1* (3-Phosphoglycerate Kinase), 36.9% for *ENO1* (Enolase), and 29.9% for *PYK1* (Pyruvate Kinase). In pentose phosphate pathway we also observed a similar regulatory pattern in *ZWF1* (Glucose-6-Phosphate Dehydrogenase), *TKL2* (Transketolase) and *NQM1* (Transaldolase). We next found that the TEs of *ADH1* (Alcohol Dehydrogenase) and *ACS1* (Acetyl-CoA Synthetase) were down-regulated, indicating that metabolic activity from ethanol to Acetyl-CoA is reduced in *puf3Δ* strain. It is well known that Acetyl-CoA directly reacts with oxaloacetic acid to generate citrate (Lian et al. 2014), which suggests that reduced biosynthesis of Acetyl-CoA in the *puf3Δ* strain could limit the metabolic flux entering the TCA cycle. This is consistent with the observation that all catalytic enzymes involved in the TCA cycle are significantly down-regulated as measured by TE (in *puf3Δ*, the relative TEs are 16.8% for *ACO1* (Aconitate Hydratase), 29.0% for *IDH1* (Isocitrate Dehydrogenase),

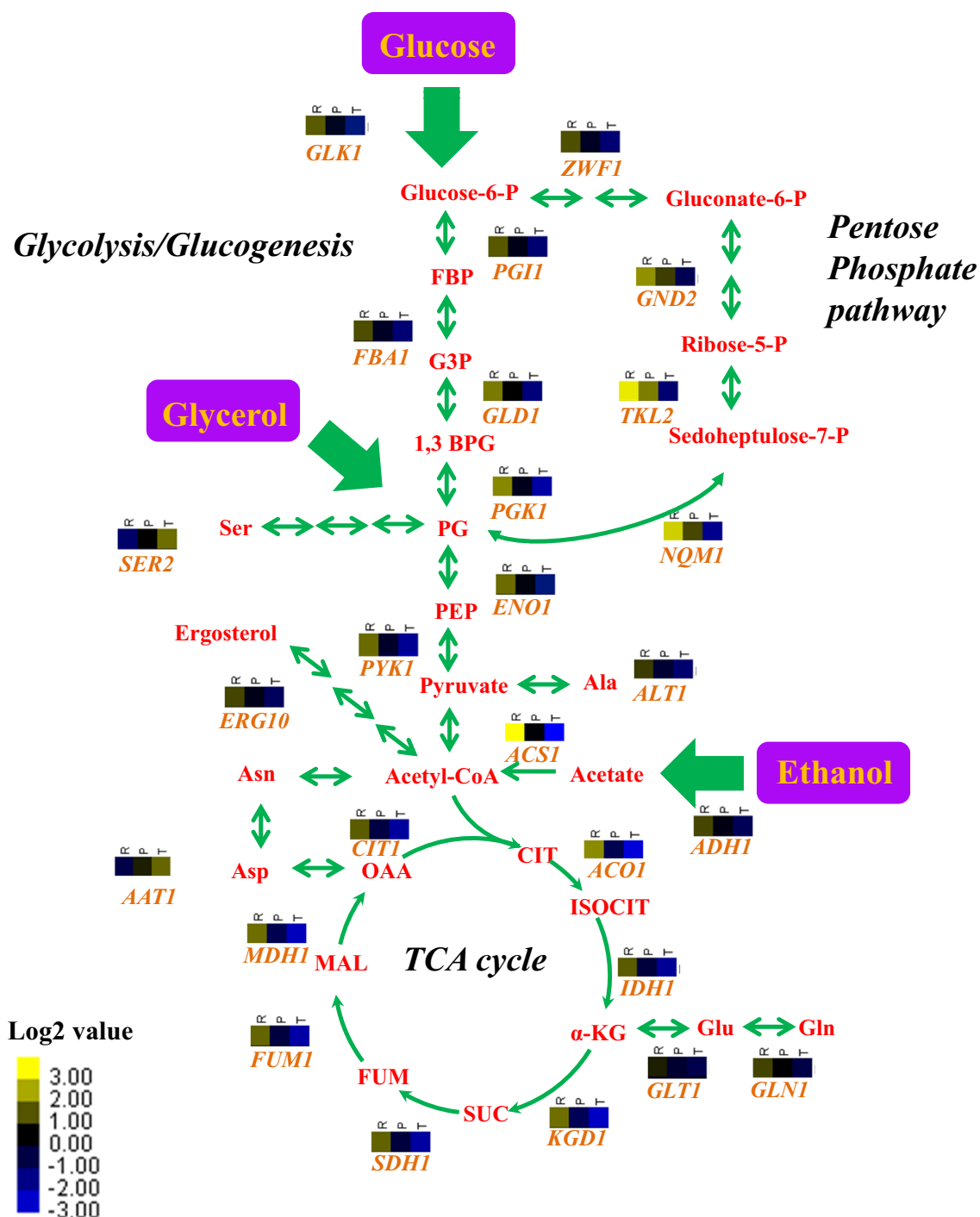


Fig. 3 The regulatory roles of Puf3p in central carbon metabolism. The metabolic structure was drawn based on KEGG (<http://www.genome.jp/kegg/>). In the labels for each detected enzyme, “R” refers to the relative change from RNA-Seq data, “P” refers to the relative change from Ribo-Seq, and “T” refers to the relative change in TE. Yellow in the heatmap denotes up-regulation, while blue represents down-regulation. For the metabolites (red fonts), the abbreviations represent: Glucose-6-P (Glucose 6-phosphate), Gluconate-6-P (Gluconate 6-phosphate), Ribose-5-P (Ribose 5-phosphate), Sedoheptu-

lose-7-P (Sedoheptulose 7-phosphate), FBP (Fructose 1,6-bisphosphate), G3P (Glyceraldehyde 3-phosphate), 1,3 BPG (Glycerate 1,3-diphosphate), PG (Phosphoglycerate), PEP (Phosphoenolpyruvate), PYR (Pyruvate), Acetyl-CoA (Acetyl Coenzyme A), Ser (Serine), Ala (Alanine), Asn (Asparagine), Asp (Aspartate), Glu (Glutamate), Gln (Glutamine), CIT (Citrate), ISOCIT (iso-Citrate), a-KG (alpha-Ketoglutarate), SUC (Succinate), FUM (Fumarate), MAL (Malate), OAA (Oxaloacetate)

19.8% for *KGD1* (alpha-Ketoglutarate Dehydrogenase), 49.9% for *SDHI* (Succinate Dehydrogenase), 25.9% for *FUM1* (Fumarate Hydratase), 21.3% for *MDH1* (Malate Dehydrogenase), and 27.6% for *CIT1* (Citrate Synthase)).

In addition, Puf3p plays a role in the regulation of a specific group of amino acids. For example, *SER2* (Phosphoserine Phosphatase) catalyzes the conversion of 3-phosphoserine to L-serine, a key step in serine biosynthesis which is upregulated after Puf3p depletion. The absence of Puf3p also increases the TE of *AAT1* (Aspartate Aminotransferase) which is responsible for catalyzing the interconversion of aspartate and α -ketoglutarate to oxaloacetate and glutamate. However, the regulation of a subset of key enzymes responsible for other amino acids in the TCA cycle, such as *GLT1* (Glutamate Synthetase), *GLN1* (Glutamine Synthetase) and *ALT1* (Alanine Transaminase), is likely independent of Puf3p's mode-of-action.

Functional enrichment analysis of the *puf3Δ* strain revealed that genes with decreased TEs were also significantly associated with oxidoreductase activity (GO: 0016491, P value = $5.20E-12$) (Table 2). Genes with oxidoreductase activity are responsible for the catalysis of oxidation–reduction reactions, and the translation levels of these genes have been shown to determine the real-time redox status of living cells rapidly. Interestingly, five genes with isocitrate dehydrogenase activity were also significantly down-regulated (GO: 0004448, P value = $7.24E-3$). These enzymes, such as *IDH1* and *IDH2*, are in charge of the catalysis of isocitrate to 2-oxoglutarate in the TCA cycle (Parker and Metallo 2015), which also implies that the function of Puf3p is important to maintain cellular energy homeostasis for oxidation–reduction balance.

Puf3 shifts mitochondrial and cytosolic ribosome biogenesis during metabolic adaptation

The regulation of translational machinery can cause global changes in TE. In eukaryotes, such as the budding yeast, the genome encodes two sets of regulatory systems to orchestrate assembly of cytosolic and mitochondrial ribosomes, respectively (Herrmann et al. 2013; Couvillion et al. 2016) (Fig. 4a). Many factors contribute to the activity of translation machinery, such as cellular energy status (intracellular ATP and GTP pool sizes) (Voorhees and Ramakrishnan 2013), substrate availability (such as tRNAs and amino acid pools) (Vambutas et al. 1991), as well as proteins that assist in translation initiation, elongation, and termination. As expected, our results demonstrate that in the *puf3Δ* strain, the TEs of mitochondrial ribosome large subunits (MLS) and small subunits (MSS) are both down-regulated, indicating that Puf3p is important for the cellular respiratory process (Fig. 4b, c). However, to our great surprise, the TEs of both cytosolic ribosome large subunits (CLS) and small

subunits (CSS) are up-regulated in the *puf3Δ* strain (Fig. 4b, c), comparing to the results of MLS, MSS and the all gene list (Supplementary Fig. 10). This result is very interesting: in negative sample groups (WT and *puf4Δ* strains, in YPD medium), above patterns are totally absent (Fig. 4d, e). It is well known that yeast slowdown in growth and, therefore, down-regulate the biogenesis of cytosolic ribosome, in respiratory growth conditions. It is interesting to observe that Puf3p can regulate this key process, indicating that Puf3p can function as a switch to down-regulate cytosolic ribosome biogenesis but enhance mitochondrial ribosome biogenesis during oxidative growth, and improve respiration-dependent energy processes during metabolic adaptation.

Discussion

From a biochemical perspective, Crabtree-positive yeasts, such as *S. cerevisiae*, predominantly rely on the rapid turnover of the glycolytic pathway, rather than respiration, when enough glucose is available (Diaz-Ruiz et al. 2011; Pfeiffer and Morley 2014; Hagman and Piškur 2015). However, alternative metabolic programs are also encoded in their genomes, to enable adaptation to fluctuations in nature, during which only non-fermentative carbon sources such as ethanol exist. From a metabolic perspective, ethanol is first converted to Acetyl-CoA, which then fuels the TCA cycle and electron transport chain under such conditions. In eukaryotic cells, this critical metabolic switch takes place in the mitochondria and requires functional synchronization among hundreds of genes. Investigating the molecular mechanisms underlying this metabolic program is essential for understanding the regulation of mitochondrial functions.

Recent evidence highlights the breadth, significance, and complexity of RBP-mediated post-transcriptional gene regulatory networks (Mittal et al. 2011). Among them, one Pumilio protein, Puf3p (homolog of mammalian PUM), is one of the most well-characterized RBPs due to its unique role in cellular respiration, a critical process for bioenergetic production and maintenance of energy homeostasis. It has been reported that over 87% of Puf3p mRNA targets were assigned to mitochondrial function by GO annotation (Gerber et al. 2004). Many of these mitochondria-associated mRNA targets encode components of the large and small mitochondrial ribosome subunits, which suggests a strong connection between Puf3p and mitochondrial protein biosynthesis. In this study, we combined Ribo-Seq and RNA-Seq with the goal of describing the landscape of Puf3p function in respiratory growth conditions. Considering that Puf3p could differentially regulate mRNA abundance and translation activity, we adapted a parameter termed Translation Efficiency (TE) to define the efficiency of a transcript generating an encoded protein. Our results

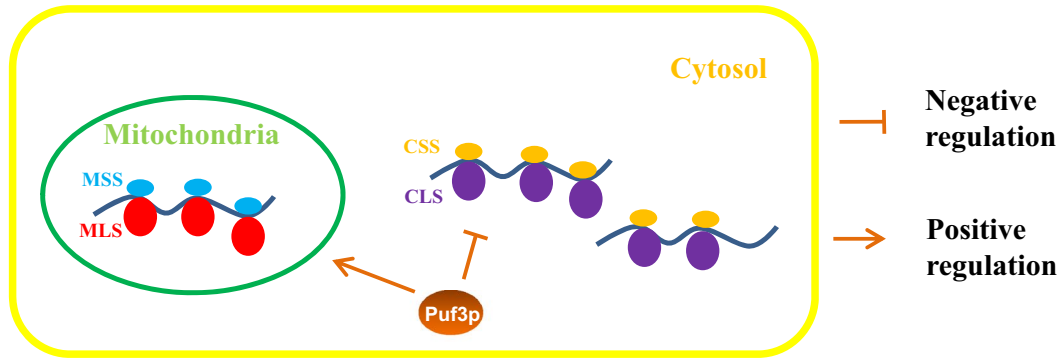
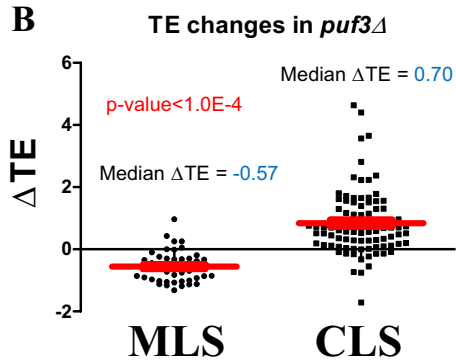
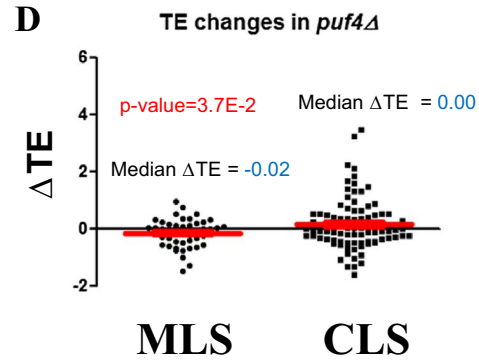
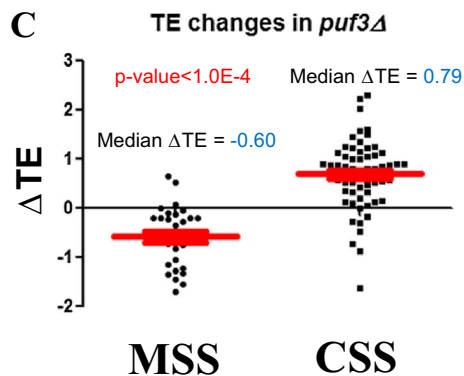
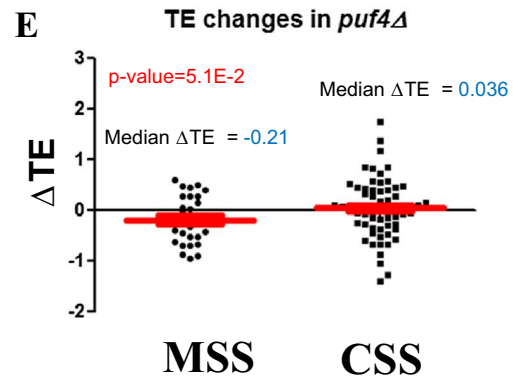
A Yeast cell**B****D****C****E**

Fig. 4 Puf3p switches the balance between mitochondrial and cytosolic ribosome biogenesis. **a** A schematic diagram indicating the two sets of ribosome machinery in eukaryotes. **b** A comparison of TE changes for mitochondrial ribosome large subunits (MLS) and cytosolic ribosome large subunits (CLS), in *puf3Δ* yeast (YPEG medium). **c** A comparison of TE changes for mitochondrial ribosome small subunits (MSS) and cytosolic ribosome small subunits (CSS),

in *puf3Δ* yeast (YPEG medium). **d** A comparison of TE changes for mitochondrial ribosome large subunits (MLS) and cytosolic ribosome large subunits (CLS), in *puf4Δ* yeast (YPD medium). **e** A comparison of TE changes for mitochondrial ribosome small subunits (MSS) and cytosolic ribosome small subunits (CSS), in *puf4Δ* yeast (YPD medium)

demonstrated that a surprisingly large fraction of genes (> 27% of overall genes) were regulated at the level of translation. An interesting observation is, most of these Puf3p translational regulated genes do not have Puf3p

binding motif, thus they could be modulated indirectly by Puf3p. As we have shown in this study, Puf3p actually is a key regulator of a post-transcriptional network including at least 65 RBPs. Therefore, Puf3p may rely on this

hierarchical structure to impose its effect on over 1000 target genes in yeast genome.

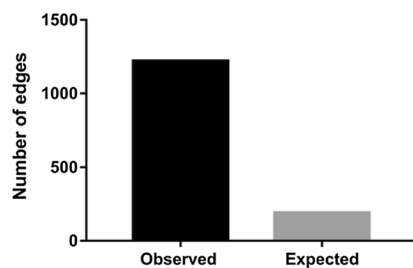
We observed a significant impact of Puf3p on the translational efficiency of enzymes involved in central carbon metabolism. It is well known that the TCA cycle is tightly linked to glycolysis (the fermentation process) (Gopalakrishnan and Maranas 2015). Many of the key enzymes are positively regulated at the translational level by Puf3p. Since most of these enzymes were not identified as Puf3p binding targets from previous RIP-ChIP experiments (Gerber et al. 2004), these newly identified genes could be direct Puf3p targets in the respiratory conditions we used in this study or maybe under indirect regulation. The result is interesting since the glycolysis pathway normally has already been down-regulated in transcription level under non-fermentative condition. However, why their TEs are also needed to be next tightly controlled by Puf3p? One of the explanations could be, under the low nutrient condition cell has to accurately lead all of possible metabolic fluxes into the more efficient TCA cycle (generate 36 ATP molecules) and avoid the possible waste in glycolysis (only generate 2 ATP molecules). Therefore, Puf3p enables reprogramming of the metabolic circuitry between fermentation and respiration. Interestingly, consistent with this, Puf3p can also leverage the balance between rates of mitochondrial and cytosolic ribosome protein synthesis. This novel connection indicates that Puf3p can act as a critical molecular switch that regulates flux between mitochondrial and cytosolic ribosome biogenesis to enable organismal adaptation to metabolic environments. It will be interesting to investigate further the molecular mechanisms underlying this regulation.

Previous studies show that genes with similar patterns of co-expression exhibit greater probability to interact at the protein level suggests that functional pathways are likely connected through Protein–Protein Interactions

(PPIs) (Grigoriev 2001; Jansen et al. 2002). However, these reported researchers mostly depended on Microarray or RNA-Seq data for the calculation of co-expression patterns (Grigoriev 2001; Jansen et al. 2002; Yu et al. 2013). In this study, we decided to test the possible correlation between coordinated TE with the extent of PPIs. Based on previous RIP-ChIP experiments (Gerber et al. 2004), we analyzed the TE of 220 direct Puf3p binding targets. Among them, the TEs of 114 target genes (with adjusted P value ≤ 0.05) are positively regulated, whereas 27 target genes (with adjusted P value ≤ 0.05) are negatively regulated by Puf3p. These genes were selected to conduct PPI analysis using the STRING 10.0 software. When we set the confidence score ≥ 0.4 as the threshold, the target genes positively regulated by Puf3p at the TE level (Supplementary Fig. 11A) appear to form many more PPIs than the null expectation (totally 1221 times, a 6.4-fold increase, the PPI enrichment P value = $2.2E-16$, Fig. 5a). Although there are only 27 target genes whose TE are negatively regulated by Puf3p (Supplementary Fig. 11B), these genes also have more PPI than expected (totally 14 times, a sevenfold increase, the PPI enrichment P value = $3.5E-7$, Fig. 5b). Therefore, Puf3p might have the ability to coordinate TEs for a specific group of genes that tend to form protein complexes for biological functions.

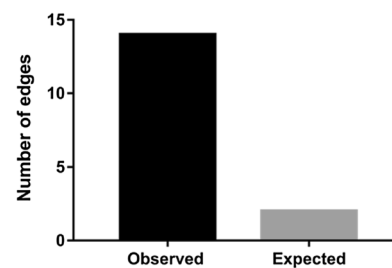
In summary, Puf3p is an important regulator of translational regulation when yeast cells undergo cellular respiration in the presence of non-fermentative nutrient sources. Partially through a network of RBP regulation, Puf3p promotes the translation of respiration-related genes and also switches the balance between mitochondrial and cytosolic ribosome biogenesis fluxes to achieve metabolic adaptation. Our investigation of Puf3p, by quantifying whole-genome transcription and translation, provides

A PPI of Puf3p positively regulated binding targets



PPI enrichment p-value < $2.2 E-16$

B PPI of Puf3p negatively regulated binding targets



PPI enrichment p-value < $3.5 E-7$

Fig. 5 Puf3p's impact on TE is related to protein–protein interactions. The Protein–Protein Interaction (PPI) analysis was conducted using the online software STRING 10.0 (<http://stringdb.org/>). The database was searched using the protein names for the two groups of Puf3p targets. The search was performed using confidence score ≥ 0.4 as the

threshold. **a** The number of observed and expected edges in the constructed PPI network for the above 114 target genes. **b** The number of observed and expected edges in the constructed PPI network for the above 27 target genes

novel insights for understanding Puf3p's functional roles in maintaining cellular energy homeostasis.

Materials and methods

Yeast strains and growth condition

S. cerevisiae strains BY4741 (MATa, *his3Δ1*, *leu2Δ0*, *met15Δ0*, *ura3Δ0*) and the single gene knockout strain *puf3Δ* in a BY4741 background were used in this study. To investigate the biological function of PUF protein, *puf3Δ* and wild-type strains were cultured in YPEG and YPD liquid medium (containing 2% Glycerol and 3% Ethanol) at 30 °C and 200 rpm.

Ribo-Seq and RNA-Seq

The yeast Ribo-Seq and RNA-Seq protocols were adapted from previously published methods (Wang et al. 2015; Sun et al. 2016). BY4741 wild-type and *puf3Δ* strains were first grown in YPD liquid medium to saturation, then both strains were transferred to YPEG or YPD medium with initial $OD_{600} = 0.1$, and harvested when OD_{600} reached 0.6–0.8. Cells were immediately treated with cycloheximide (CHX, to a final concentration at 100 µg/ml) for 2 min to inhibit the cytosolic translation. Cell pellets were then divided into two parts. RNA was extracted from one part by hot phenol method (Zhong et al. 2011) and RNA was subsequently used for RNA-Seq. Two biological replicates were conducted for each sample.

The other part was used for Ribo-seq analysis using a previously published protocol (Ingolia et al. 2009). In brief, the cell pellet was treated with 2.5 ml polysome lysis buffer [20 mM Tris–Cl (pH 8.0), 140 mM KCl, 1.5 mM MgCl₂, 100 µg/ml CHX, 1% (v/v) Triton X-100] and ground in a mortar with liquid nitrogen. After thawing the cell powder at 30 °C for 2 min, the cell pellet was centrifuged at 3,000×g at 4 °C for 5 min to remove cell debris. The supernatant was cleared by another centrifugation step at 20,000×g at 4 °C for 10 min. The cell extract was diluted to $A_{260} = 200$ with polysome lysis buffer.

To obtain the monosome fraction, 7.5 µl RNase I (Ambion, AM2294) was added to 250 µl cell extract for 1 h's reaction at 25 °C, which was then stopped by applying 5 µl SUPERase.In (Ambion, AM2694). Afterwards, the 80S monosome fraction was collected from the cell extract using sucrose density gradients (centrifuged at 35,000 rpm at 4 °C for 3 h). The standard SDS/phenol method was utilized to purify the footprint fragments, and then the protected RNA fragments were dephosphorylated at their 3' ends by the T4 polynucleotide kinase. Polyacrylamide denaturing gel purification was conducted to purify the mRNA footprint

fragments. The region near the 28 nt marker was excised. RNA was recovered from the gel slice and quantified by BioAnalyzer (Agilent). A poly-A tail was added to each RNA fragment by *E. coli* poly-A polymerase (NEB, M0276S), and then reverse transcription was conducted with primers that are linked to unique barcodes. 10% denaturing polyacrylamide gel was used to purify the reverse transcription products, the range between 90 and 130 nucleotides was excised and cDNA fragments were recovered.

To construct the sequencing library, CircLigase (Epicentre Biotechnologies CL4111K) was added to the gel extraction products and the mixtures were incubated at 60 °C for 1 h, and then heated at 80 °C for 10 min to inactivate the reaction. Afterwards, the circularized DNA was used as the template for amplification by Phusion polymerase for 12 cycles, and 8% non-denaturing polyacrylamide gel was utilized to purify the PCR products. The PCR products at about 120 bp were eventually recovered from the excised gel slice, and quantified by BioAnalyzer (Agilent, 2100). Finally, the Illumina HiSeq2000 platform (50 bp, single-end) was adapted to perform the deep sequencing. Two biological replicates were conducted for each sample.

Read mapping and transcription/translation quantification

Read mapping and transcription/translation quantification generally followed previously published protocols (Wang et al. 2015; Sun et al. 2016). The raw reads from the Ribo-Seq were processed by removing the terminal polyA sequences and then selecting reads ranging from 16 to 35 bp long. The rRNA sequences were next removed using bowtie (Langmead 2010). The rest of the reads were aligned to the *S. cerevisiae* genome with the criteria of less than two mismatches. Quantification of gene transcription and translation was performed by the DESeq package (Anders and Huber 2010). Translation Efficiency (TE) was calculated from the RFP/mRNA. The *P* value was adjusted by the Benjamini-Hochberg method to control the false discovery rate (FDR). The criteria of adjusted $P \leq 0.05$ and $\log_2(\text{fold change}) \geq 1$ were used throughout the paper.

Gene ontology (GO) enrichment analysis and statistics

The Gene Ontology (GO) analysis was performed using the online software Gene Ontology Term Finder (<http://www.yeastgenome.org/cgi-bin/GO/goTermFinder.pl>). GO Term Finder calculates a *P* value using the hypergeometric distribution. We used a *P* value cut off of 0.01 to define statistical enrichment. The whole gene list of budding yeast (7164 genes in total) was used as the background set. The list of

genes with significantly changed TE was used as the query set.

Protein–protein interaction analysis

A protein–protein interaction (PPI) analysis was conducted using the web version of STRING 10.0 (available at <http://stringdb.org/>) (Szklarczyk et al. 2015). The database was searched using gene names discussed in the text. The search was performed by setting the confidence score ≥ 0.4 as the threshold (which was reported before as the medium confidence range von Mering et al. 2005). The edges in the network represent protein–protein interactions reported in the database using experimental evidence or predicted by the algorithm of STRING 9.1 (Franceschini et al. 2013). The software chose a random background model that preserves the degree distribution of the tested proteins in a given list, and tested the significance of the observed PPI. The detailed computational procedures have been reported in previous literature (Maslov and Sneppen 2002).

Data access

All raw RNA-Seq AND Ribo-Seq data have been submitted to the Sequence Read Archive of NCBI. The accession numbers are SRR1177847–SRR1177850, SRR5483532–SRR5483533 and SRR5483539.

Acknowledgements This work was supported by various funds from Cornell University, and National Institutes of Health [R01GM117190] to Z. Gu. The authors are grateful to Mr. Yiping Wang for reading the manuscript.

Author contributions Zhe Wang designed and conducted ribosome profiling studies. Xuepeng Sun and Zhe Wang analyzed the ribosome profiling data. Zhe Wang and Xiaoxian Guo designed and conducted RNA-seq studies. Zhe Wang, Josephine Wee and Zhenglong Gu wrote the manuscript. Zhenglong Gu initiated and directed this research.

Compliance with ethical standards

Conflict of interest The authors declare no competing financial interests.

References

Anders S, Huber W (2010) Differential expression analysis for sequence count data. *Genome Biol* 11:R106. <https://doi.org/10.1186/gb-2010-11-10-r106>

Blackinton JG, Keene JD (2014) Post-transcriptional RNA regulons affecting cell cycle and proliferation. *Semin Cell Dev Biol* 34:44–54. <https://doi.org/10.1016/j.semcdb.2014.05.014>

Brar GA, Yassour M, Friedman N et al (2012) High-resolution view of the yeast meiotic program revealed by ribosome profiling. *Science* 335:552–557. <https://doi.org/10.1126/science.1215110>

Chatenay-Lapointe M, Shadel GS (2011) Repression of mitochondrial translation, respiration and a metabolic cycle-regulated gene, SLF1, by the yeast Pumilio-family protein Puf3p. *PLoS One*. <https://doi.org/10.1371/journal.pone.0020441>

Couvillion MT, Soto IC, Shipkovenska G, Churchman LS (2016) Synchronized mitochondrial and cytosolic translation programs. *Nature* 533:1–17. <https://doi.org/10.1038/nature18015>

Defenouillère Q, Fromont-Racine M (2017) The ribosome-bound quality control complex: from aberrant peptide clearance to proteostasis maintenance. *Curr Genet* 63:997–1005. <https://doi.org/10.1007/s00294-017-0708-5>

Diaz-Ruiz R, Rigoulet M, Devin A (2011) The Warburg and Crabtree effects: on the origin of cancer cell energy metabolism and of yeast glucose repression. *Biochim Biophys Acta Bioenerg* 1807:568–576. <https://doi.org/10.1016/j.bbabi.2010.08.010>

Eliyahu E, Pnueli L, Melamed D et al (2010) Tom20 mediates localization of mRNAs to mitochondria in a translation-dependent manner. *Mol Cell Biol* 30:284–294. <https://doi.org/10.1128/MCB.00651-09>

Evans CR, Ling J (2017) Visualizing translational errors: one cell at a time. *Curr Genet* 64:1–4. <https://doi.org/10.1007/s00294-017-0784-6>

Franceschini A, Szklarczyk D, Frankild S et al (2013) STRING v9.1: protein-protein interaction networks, with increased coverage and integration. *Nucleic Acids Res* 41:D808–D815. <https://doi.org/10.1093/nar/gks1094>

Freeberg MA, Han T, Moresco JJ et al (2013) Pervasive and dynamic protein binding sites of the mRNA transcriptome in *Saccharomyces cerevisiae*. *Genome Biol* 14:R13. <https://doi.org/10.1186/gb-2013-14-2-r13>

Gadir N, Haim-Vilmovsky L, Kraut-Cohen J, Gerst JE (2011) Localization of mRNAs coding for mitochondrial proteins in the yeast *Saccharomyces cerevisiae*. *Rna* 17:1551–1565. <https://doi.org/10.1261/rna.2621111.2>

Gerber AP, Herschlag D, Brown PO (2004) Extensive association of functionally and cytotopically related mRNAs with Puf family RNA-binding proteins in yeast. *PLoS Biol* 2:e79. <https://doi.org/10.1371/journal.pbio.0020079>

Gopalakrishnan S, Maranas CD (2015) 13C metabolic flux analysis at a genome-scale. *Metab Eng* 32:12–22. <https://doi.org/10.1016/j.ymben.2015.08.006>

Grigoriev a (2001) A relationship between gene expression and protein interactions on the proteome scale: analysis of the bacteriophage T7 and the yeast *Saccharomyces cerevisiae*. *Nucleic Acids Res* 29:3513–3519. <https://doi.org/10.1093/nar/29.17.3513>

Gupta I, Clauder-Münster S, Klaus B et al (2014) Alternative polyadenylation diversifies post-transcriptional regulation by selective RNA-protein interactions. *Mol Syst Biol* 10:719. <https://doi.org/10.1002/msb.135068>

Hagman A, Piškur J (2015) A study on the fundamental mechanism and the evolutionary driving forces behind aerobic fermentation in yeast. *PLoS One* 10:e0116942. <https://doi.org/10.1371/journal.pone.0116942>

He F, Jacobson A (2017) NMD monitors translational fidelity 24/7. *Curr Genet* 63:1007–1010. <https://doi.org/10.1007/s00294-017-0709-4>

Herrmann JM, Woellhaf MW, Bonnefoy N (2013) Control of protein synthesis in yeast mitochondria: The concept of translational activators. *Biochim Biophys Acta Mol Cell Res* 1833:286–294. <https://doi.org/10.1016/j.bbamcr.2012.03.007>

Houshmandi SS, Olivas WM (2005) Yeast Puf3 mutants reveal the complexity of Puf-RNA binding and identify a loop required for regulation of mRNA decay. *RNA* 11:1655–1666. <https://doi.org/10.1261/rna.2168505>

- Imig J, Kanitz A, Gerber AP (2012) RNA regulons and the RNA-protein interaction network. *Biomol Concepts* 3:403–414. <https://doi.org/10.1515/bmc-2012-0016>
- Ingolia NT, Ghaemmaghami S, Newman JRS, Weissman JS (2009) Genome-wide analysis in vivo of translation with nucleotide resolution using ribosome profiling. *Science* 324:218–223. <https://doi.org/10.1126/science.1168978>
- Ingolia NT, Brar G, Rouskin S et al (2013) Genome-wide annotation and quantitation of translation by ribosome profiling. *Curr Protoc Mol Biol*. <https://doi.org/10.1002/0471142727.mb0418s103>
- Jackson JS, Houshmandi SS, Lopez Leban F, Olivas WM (2004) Recruitment of the Puf3 protein to its mRNA target for regulation of mRNA decay in yeast. *RNA* 10:1625–1636. <https://doi.org/10.1261/rna.7270204>
- Jansen R, Greenbaum D, Gerstein M (2002) Relating whole-genome expression data with protein-protein interactions. *Genome Res* 12:37–46. <https://doi.org/10.1101/gr.205602.4>
- Jiang H, Guan W, Gu Z (2010) Tinkering evolution of post-transcriptional RNA regulons: Puf3p in fungi as an example. *PLoS Genet* 6:e1001030. <https://doi.org/10.1371/journal.pgen.1001030>
- Jiang H, Xu L, Wang Z et al (2014) Coordinating expression of RNA binding proteins with their mRNA targets. *Sci Rep* 4:7175. <https://doi.org/10.1038/srep07175>
- Keene J (2007) RNA regulons: coordination of post-transcriptional events. *Nat Rev Genet* 8:533–543. <https://doi.org/10.1038/nrg2111> doi
- Kennedy BK, Gotta M, Sinclair D et al (1997) Redistribution of silencing proteins from telomeres to the nucleolus is associated with extension of life span in *S. cerevisiae*. *Cell* 89:381–391. [https://doi.org/10.1016/S0092-8674\(00\)80219-6](https://doi.org/10.1016/S0092-8674(00)80219-6)
- Kershaw CJ, Costello JL, Talavera D et al (2015) Integrated multi-omics analyses reveal the pleiotropic nature of the control of gene expression by Puf3p. *Sci Rep* 5:15518. <https://doi.org/10.1038/srep15518>
- Langmead B (2010) Aligning short sequencing reads with bowtie. *Curr Protoc Bioinforma*. <https://doi.org/10.1002/0471250953.bi1107s32>
- Lee C-D, Tu BP (2015) Glucose-regulated phosphorylation of the PUF Protein Puf3 regulates the translational fate of its bound mRNAs and association with RNA granules. *Cell Rep* 11:1638–1650. <https://doi.org/10.1016/j.celrep.2015.05.014>
- Lee D, Ohn T, Chiang Y-C et al (2010) PUF3 acceleration of deadenylation in vivo can operate independently of CCR4 activity, possibly involving effects on the PAB1-mRNP structure. *J Mol Biol* 399:562–575. <https://doi.org/10.1016/j.jmb.2010.04.034>
- Lian J, Si T, Nair NU, Zhao H (2014) Design and construction of acetyl-CoA overproducing *Saccharomyces cerevisiae* strains. *Metab Eng* 24:139–149. <https://doi.org/10.1016/j.ymben.2014.05.010>
- Maslov S, Sneppen K (2002) Specificity and stability in topology of protein networks. *Science* 296:910–913. <https://doi.org/10.1126/science.1065103>
- Miller M, Russo J, Fischer AD et al (2014) Carbon source-dependent alteration of Puf3p activity mediates rapid changes in the stabilities of mRNAs involved in mitochondrial function. *Nucleic Acids Res* 42:3954–3970. <https://doi.org/10.1093/nar/gkt1346>
- Mittal N, Scherrer T, Gerber AP, Janga SC (2011) Interplay between posttranscriptional and posttranslational interactions of RNA-binding proteins. *J Mol Biol* 409:466–479. <https://doi.org/10.1016/j.jmb.2011.03.064>
- Morris DR (2009) Ribosomal footprints on a transcriptome landscape. *Genome Biol* 10:215. <https://doi.org/10.1186/gb-2009-10-4-215>
- Olivas W, Parker R (2000) The Puf3 protein is a transcript-specific regulator of mRNA degradation in yeast. *EMBO J* 19:6602–6611. <https://doi.org/10.1093/emboj/19.23.6602>
- Parker SJ, Metallo CM (2015) Metabolic consequences of oncogenic IDH mutations. *Pharmacol Ther* 152:54–62. <https://doi.org/10.1016/j.pharmthera.2015.05.003>
- Pfeiffer T, Morley A (2014) An evolutionary perspective on the Crabtree effect. *Front Mol Biosci* 1:1–6. <https://doi.org/10.3389/fmolb.2014.00017>
- Pop C, Rouskin S, Ingolia NT et al (2014) Causal signals between codon bias, mRNA structure, and the efficiency of translation and elongation. *Mol Syst Biol* 10:770. <https://doi.org/10.1525/msb.20145524>
- Riordan DP, Herschlag D, Brown PO (2011) Identification of RNA recognition elements in the *Saccharomyces cerevisiae* transcriptome. *Nucleic Acids Res* 39:1501–1509. <https://doi.org/10.1093/nar/gkq920>
- Rowe W, Kershaw CJ, Castelli LM et al (2014) Puf3p induces translational repression of genes linked to oxidative stress. *Nucleic Acids Res* 42:1026–1041. <https://doi.org/10.1093/nar/gkt948>
- Scherrer T, Mittal N, Janga SC, Gerber AP (2010) A screen for RNA-binding proteins in yeast indicates dual functions for many enzymes. *PLoS One* 5:e15499. <https://doi.org/10.1371/journal.pone.0015499>
- Sun X, Wang Z, Guo X et al (2016) Coordinated evolution of transcriptional and post-transcriptional regulation for mitochondrial functions in yeast strains. *PLoS One* 11:e0153523. <https://doi.org/10.1371/journal.pone.0153523>
- Szklarczyk D, Franceschini A, Wyder S et al (2015) STRING v10: protein-protein interaction networks, integrated over the tree of life. *Nucleic Acids Res* 43:D447–D452. <https://doi.org/10.1093/nar/gku1003>
- Vambutas A, Ackerman SH, Tzagoloff A (1991) Mitochondrial translational-initiation and elongation factors in *Saccharomyces cerevisiae*. *Eur J Biochem* 201:643–652. <https://doi.org/10.1111/j.1432-1033.1991.tb16325.x>
- von Mering C, Jensen LJ, Snel B et al (2005) STRING: known and predicted protein-protein associations, integrated and transferred across organisms. *Nucleic Acids Res* 33:433–437. <https://doi.org/10.1093/nar/gki005>
- Voorhees RM, Ramakrishnan V (2013) Structural basis of the translational elongation cycle*. *Annu Rev Biochem* 82:203–236. <https://doi.org/10.1146/annurev-biochem-113009-092313>
- Wang X, McLachlan J, Zamore PD, Hall TMT (2002) Modular recognition of RNA by a human pumilio-homology domain. *Cell* 110:501–512. [https://doi.org/10.1016/S0092-8674\(02\)00873-5](https://doi.org/10.1016/S0092-8674(02)00873-5)
- Wang Z, Sun X, Zhao Y et al (2015) Evolution of gene regulation during transcription and translation. *Genome Biol Evol* 7:1155–1167. <https://doi.org/10.1093/gbe/evv059>
- Wickens M, Bernstein DS, Kimble J, Parker R (2002) A PUF family portrait: 3'UTR regulation as a way of life. *Trends Genet* 18:150–157. [https://doi.org/10.1016/S0168-9525\(01\)02616-6](https://doi.org/10.1016/S0168-9525(01)02616-6)
- Yu F-D, Yang S-Y, Li Y-Y, Hu W (2013) Co-expression network with protein-protein interaction and transcription regulation in malaria parasite *Plasmodium falciparum*. *Gene* 518:7–16. <https://doi.org/10.1016/j.gene.2012.11.092>
- Zhang B, Gallegos M, Puoti A et al (1997) A conserved RNA-binding protein that regulates sexual fates in the *C. elegans* hermaphrodite germ line. *Nature* 390:477–484. <https://doi.org/10.1038/37297>
- Zhong S, Joung J-G, Zheng Y et al (2011) High-throughput illumina strand-specific RNA sequencing library preparation. *Cold Spring Harb Protoc*. <https://doi.org/10.1101/pdb.prot5652>